Chemical Control of Hole Distribution and Superconductivity in $(Cu,Mo)Sr_2(Ce,R)_sCu_2O_{5+2s+\delta}$ ($s = 2, 3$; R = Y, La−Yb)

I. Grigoraviciute,[†] J. M. Chen,[‡] R. S. Liu,[§] S. Ishii,[†] H. Yamauchi,[†] and M. Karppinen*[,†,||]

Materials and Structures Laboratory, Tokyo Institute of Technology, Yokohama 226-8503, Japan, National Synchrotron Radiation Research Center (NSRRC), Hsinchu 30076, Taiwan, Republic of China, Department of Chemistry, National Taiwan University, Taipei 106, Taiwan, Republic of China, and Laboratory of Inorganic and Analytical Chemistry, Helsinki University of Technology, Espoo 02150, Finland

Received August 7, 2006. Revised Manuscript Received October 13, 2006

In the crystal structure of members of the $(Cu,Mo)Sr_2(Ce,R)_sCu_2O_{5+2s+\delta}$ or (Cu,Mo)-12*s*2 homologous series of superconductive copper oxides, adjacent CuO_2 planes are separated by a fluorite-structured (Ce,R)-$[O_2$-$(Ce,R)]_{s-1}$ blocking block. Here we utilize the fluorite block as a "chemical-pressure medium" for the $s = 2$ and 3 members of the series. The (Ce,R) sites readily accommodate rare earth elements (R) ranging in size from La down to Yb. With decreasing size of the R constituent, T_c first monotonically increases and then decreases, having a maximum around R = Y for both $s = 2$ and $s = 3$. At the same time the average valence of copper, derived for the $s = 2$ samples from Cu L_3-edge XANES spectra, is found to remain constant at 2.20 ± 0.01. An explanation for the unique chemical-pressure effect is revealed from O K-edge XANES spectra, the resolution of which allows us to distinguish the CuO_2 plane holes from those residing in the $(Cu,Mo)O_{1+\delta}$ charge reservoir. The result shows that the T_c value and the density of CuO_2 plane holes follow parallel trends with respect to the size of R.

Introduction

"Chemical pressure" is a widely appreciated tool for fine-tuning the functional properties of multilayered oxides. A variety of examples of such chemical-pressure utility are found among, e.g., high-T_c superconductive (HTS) copper oxides and colossal magnetoresistance (CMR) manganese oxides.[1−3] Chemical pressure is generated through "isovalent smaller-for-larger" cation substitution, typically involving either divalent alkaline earth or trivalent rare earth elements. To detect pure pressure effects, the substitution should proceed such that the overall cation charge is kept constant. Therefore, an essential requirement is that the oxygen content remains constant throughout the substitution range investigated.[4] Chemical pressure is often taken as an analogue to "physical pressure".[5] However, the two pressures often act to opposite directions in complex multilayered systems.[1−3,6] Despite the widespread utilization of the pressure effects, real understanding behind the apparent outcomes of them is lacking yet.

Among HTS copper oxide phases, those having adjacent CuO_2 planes separated by rare earth (R) elements provide us with an appropriate framework for chemical-pressure studies. A common feature for such systems is that any of the R elements can be fully substituted by most of the other R elements. For the prototype HTS oxide, $CuBa_2RCu_2O_{7-\delta}$ (i.e., "R-123" or Cu-1212 with a layer sequence of BaO−$CuO_{1-\delta}$−BaO−CuO_2−R−CuO_2), T_c decreases upon decreasing the size of the R constituent,[4,7] whereas the opposite is true for the other well-known R-based system, $Cu_2Ba_2RCu_2O_{8-\delta}$ ("R-124" or Cu-2212 with a layer sequence of BaO−$CuO_{1-\delta/2}$−$CuO_{1-\delta/2}$−BaO−CuO_2−R−CuO_2).[8,9] The reason for the opposite trends has not been fully revealed yet. Here we should recognize a possibility that even though the average valence of copper remains constant upon replacing one of the R^{III} species by another, chances are that the charge balance between the $CuO_{1-\delta}$ or $Cu_2O_{2-\delta}$ charge-reservoir block and the CuO_2 planes is affected.[4,6,10] Indeed, bond-valence-sum calculations for $CuBa_2RCu_2O_{7-\delta}$ have suggested that, with decreasing size of the trivalent R constituent, part of the positive charge of the nonsuperconductive $CuO_{1-\delta}$ chain is gradually shifted to the CuO_2−R−CuO_2 block containing the superconductive CuO_2 planes.[4,6,11] Early Seebeck coefficient data for the $CuBa_2RCu_2O_{7-\delta}$

* To whom correspondence should be addressed. Fax: +81-45-924-5365. E-mail: karppinen@msl.titech.ac.jp.
[†] Tokyo Institute of Technology.
[‡] NSRRC.
[§] National Taiwan University.
[||] Helsinki University of Technology.

(1) Licci, F.; Gauzzi, A.; Marezio, M.; Radaelli, G. P.; Masini, R.; Chaillout-Bougerol, C. *Phys. Rev. B* **1998**, *58*, 15208.
(2) Toulemonde, P.; Odier, P.; Bordet, P.; Le Floch, S.; Suard, E. *J. Phys.: Condens. Matter* **2004**, *16*, 4061, 4077.
(3) Hwang, H. Y.; Cheong, S. -W.; Radaelli, P. G.; Marezio, M.; Batlogg, B. *Phys. Rev. Lett.* **1995**, *75*, 914. Radaelli, P. G.; Iannone, G.; Marezio, M.; Hwang, H. Y.; Cheong, S. W.; Jorgensen, J. D.; Argyriou, D. N. *Phys. Rev. B* **1997**, *56*, 8265.
(4) Yasukawa, Y.; Nakane, T.; Yamauchi, H.; Karppinen, M. *Appl. Phys. Lett.* **2001**, *78*, 2917.
(5) Chu, C. W.; Hor, P. H.; Meng, R. L.; Gao, L.; Huang, Z. J.; Wang, Y. Q. *Phys. Rev. Lett.* **1987**, *58*, 405.
(6) Karppinen, M.; Kiryakov, N.; Yasukawa, Y.; Nakane, T.; Yamauchi, H. *Physica C* **2002**, *382*, 66.
(7) Guillaume, M.; Allenspach, P.; Henggeler, W.; Mesot, J.; Roessli, B.; Staub, U.; Fischer, P.; Furrer, A.; Trounov, V. *J. Phys.: Condens. Matter* **1994**, *6*, 7963.
(8) Morris, D. E.; Nickel, J. H.; Wei, J. Y. T.; Asmar, N. G.; Scott, J. S.; Scheven, U. M.; Hultgren, C. T.; Markelz, A. G.; Post, J. E.; Heaney, P. J.; Veblen, D. R.; Hazen, R. M. *Phys. Rev. B* **1989**, *39*, 7347.
(9) Tatsumi, M.; Kawazoe, M.; Yamamoto, S. *Physica C* **1996**, *262*, 261.
(10) Karppinen, M.; Yamauchi, H. *Mater. Sci. Eng., R* **1999**, *26*, 844.

10.1021/cm061856r CCC: $33.50
Published on Web 11/29/2006

compounds could also be interpreted along this view.[12] Since fully oxygenated samples of the Cu-1212 phase are in a slightly overdoped state, an increase in the CuO_2 plane hole density would then cause a decrease in the T_c value, as it makes the phase more heavily overdoped.

In the newly realized (Cu,Mo)-12*s*2 or (Cu,Mo)$Sr_2(Ce,Y)_s$-$Cu_2O_{5+2s+\delta}$ homologous series of HTS copper oxides, adjacent CuO_2 planes are separated by a fluorite-structured $(Ce,Y)[O_2(Ce,Y)]_{s-1}$ block (with expected valence states of Ce^{IV} and Y^{III}) such that the phases obey a layer sequence of $SrO-(Cu,Mo)O_{1+\delta}-SrO-CuO_2-(Ce,Y)-[O_2-(Ce,Y)]_{s-1}-CuO_2$.[13] In our preceding work for the $s = 3$ member of the series, it was shown that the $(Ce,Y)-O_2-(Ce,Y)-O_2-(Ce,Y)$ block is flexible enough for Y to be fully replaced by other R constituents ranging from La to Yb.[14] Hence, the (Cu,Mo)-12*s*2 series provides us with an interesting new model system for deepening our understanding on the R-element-derived chemical-pressure effects. The present work is focused on the $s = 2$ and 3 members of the series. For sample characterization, X-ray absorption near-edge structure (XANES) spectroscopy was employed. The spectra were collected (for $s = 2$) at both Cu $L_{2,3}$- and O K-edges. The former allows relatively accurate determination of the total amount of doped holes, whereas the latter reveals their distribution between the $(Cu,Mo)O_{1+\delta}$ charge reservoir and the CuO_2 planes.

Experimental Section

Samples of the two phases $(Cu_{0.75}Mo_{0.25})Sr_2(Ce_{0.45}R_{0.55})_2Cu_2O_{9+\delta}$ [(Cu,Mo)-1222] and $(Cu_{0.75}Mo_{0.25})Sr_2(Ce_{0.67}R_{0.33})_3Cu_2O_{11+\delta}$ [(Cu,Mo)-1232], with R = La, Nd, Sm, Eu, Gd, Dy, Y, Ho, Er, Tm, and Yb, were synthesized from stoichiometric mixtures of high-purity CuO, MoO_3, $SrCO_3$, CeO_2, and R_2O_3 powders. The powder mixtures were calcined in air at 950 °C for 24 h and after careful grinding pressed into pellets for three or four consequent 24 h heat-treatment periods (with regrinding and subsequent repelletizing between them) carried out at 1020 °C in air (for the $s = 3$, R = Yb sample at 1090 °C in flowing O_2 gas[14]). For both $s = 2$ and $s = 3$, the synthesis process yielded single-phase samples within the detection limit of powder X-ray diffraction (XRD) measurement (Rigaku RINT2550VK/U equipped with a rotating Cu anode). The as-air-synthesized samples, however, are not superconductive, but an additional high-pressure oxygenation (HPO) annealing is required to induce superconductivity in the (Cu,Mo)-12*s*2 phases.[13,14] The HPO annealing was carried out in a cubic-anvil-type ultra-high-pressure apparatus at 5 GPa and 500 °C for 30 min. For the HPO annealing, a ~100 mg portion of air-synthesized sample was thoroughly mixed with 75 mol % Ag_2O_2, which acts as an efficient external oxygen source as it decomposes to Ag and/or Ag_2O in the sample cell during the high-pressure treatment. It should be mentioned that we also successfully synthesized the samples with R = Pr and Tb (for both $s = 2$ and $s = 3$) in single-phase form. However, they remained nonsuperconductive even after the HPO annealing and were therefore excluded from the scope of the present work. Furthermore, we attempted to synthesize the R = Lu phases: for $s = 3$ no phase formation was observed, whereas for $s = 2$ the synthesis yielded multiphase samples with the (Cu,Mo)-1222 phase as the main phase though. For the phase-pure samples (included in the present work), lattice parameters were readily refined from the XRD data in the tetragonal space groups *I*4/*mmm* ($s = 2$) and *P*4/*mmm* ($s = 3$).[13] Superconductivity properties of the samples were investigated using a superconducting-quantum-interface-device magnetometer (SQUID; Quantum Design MPMS-XL5) in the temperature range from 5 to 100 K under an applied field of 10 Oe in both zero-field-cooled (ZFC) and field-cooled (FC) modes. The value of T_c was taken at the onset temperature of the diamagnetic signal.

X-ray absorption spectra were collected for the oxygen-loaded (superconductive) $s = 2$ samples at both Cu $L_{2,3}$- and O K-edges in X-ray fluorescence yield mode at the 6 m HSGM beam-line of the National Synchrotron Radiation Research Center in Hsinchu, Taiwan; experimental details were as previously given elsewhere.[14,15] In brief, the spectra were recorded using a micro-channel-plate (MCP) detector system located parallel to the sample surface at a distance of ~2 cm. Photons were incident at an angle of 45° with respect to the sample normal. The incident photon flux was monitored simultaneously by a Ni mesh located after the exit slit of the monochromator. The photon energies were calibrated with an accuracy of 0.1 eV using the Cu L_3 white line at 931.2 eV and the O K-edge absorption peak at 530.1 eV of a CuO reference. The monochromator resolution was set to ~0.15 eV for the O K-edge energy region and to ~0.30 eV for the Cu L-edge energy region. The recorded spectra were corrected for the energy-dependent incident photon intensity as well as for self-absorption effects[16,17] and normalized to the tabulated standard absorption cross sections.[18]

Results and Discussion

In Figure 1, lattice parameter *c* is plotted as a function of $r(Ce^{IV},R^{III})$ (average ionic radius at the (Ce,R) site[19]) for both the air-synthesized (AS) and the HPO samples of the two phases (Cu,Mo)-1222 and (Cu,Mo)-1232. For all the R constituents a common trend is seen: oxygen loading through the HPO annealing causes the *c* parameter to contract by ~0.07 Å (per formula unit). Lattice contraction along the *c*-axis is what one commonly sees for HTS copper oxides and also what was expected from our previous work on the (Cu,Mo)-12*s*2 series.[13,14] It was rather interesting to note that the magnitude of contraction was essentially the same (within ±0.005 Å) for all the samples. This already gives a positive signal toward the fact that we apparently were able to load the samples with the same amount of (excess) oxygen. A further proof was obtained from the Cu L-edge XANES data; see the discussion later on for the (Cu,Mo)-1222 samples.

All the oxygen-loaded samples were found to exhibit bulk superconductivity. In Figure 2, the value of T_c is plotted for

(11) Samoylenkov, S. V.; Gorbenko, O. Yu Kaul, A. R. *Physica C* **1997**, *278*, 49.
(12) Kang, W. N.; Choi, M.-Y. *Phys. Rev. B* **1990**, *42*, 2573.
(13) Morita, Y.; Nagai, T.; Matsui, Y.; Yamauchi, H.; Karppinen, M. *Phys. Rev. B* **2004**, *70*, 174515. Karppinen, M.; Morita, Y.; Kobayashi, T.; Grigoraviciute, I.; Chen, J. M.; Liu, R. S.; Yamauchi, H. *J. Solid State Chem.* **2005**, *178*, 3464. Grigoraviciute, I.; Yamauchi, H.; Karppinen, M. Unpublished results, 2006.
(14) Karppinen, M.; Morita, Y.; Chen, J. M.; Liu, R. S.; Yamauchi, H. *Phys. Rev. B* **2005**, *72*, 12501.
(15) Karppinen, M.; Kotiranta, M.; Nakane, T.; Chang, S. C.; Chen, J. M.; Liu, R. S.; Yamauchi, H. *Phys. Rev. B* **2003**, *67*, 134522.
(16) Tröger, D.; Arvanitis, K.; Baberschke, H.; Michaelis, U.; Grimm, E.; Zschech, E. *Phys. Rev. B* **1992**, *46*, 3283.
(17) Pellegrin, E.; Nücker, N.; Fink, J.; Molodtsov, S. L.; Gutiérrez, A.; Navas, E.; Strebel, O.; Hu, Z.; Domke, M.; Kaindl, G.; Uchida, S.; Nakamura, Y.; Markl, J.; Klauda, M.; Saemann-Ischenko, G.; Krol, A. *Phys. Rev. B* **1993**, *47*, 3354.
(18) Yeh, J. J.; Lindau, I. *At. Data Nucl. Data Tables* **1985**, *32*, 1.
(19) Shannon, R. D. *Acta Crystallogr., Ser. A* **1976**, *32*, 751.

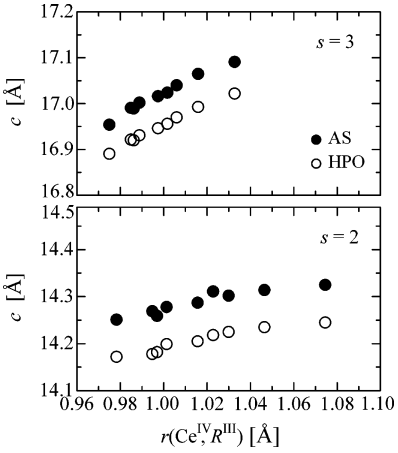

Figure 1. Lattice parameter c for AS (●) and HPO (○) samples of (Cu,Mo)-12s2 (s = 2 and 3) plotted against the average ionic radius, r(Ce^{IV},R^{III}), of the fluorite-block cations.

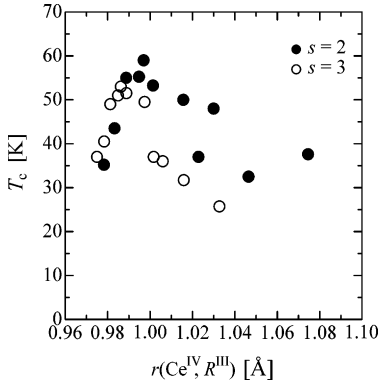

Figure 2. T_c values for similarly synthesized and high-pressure-oxygenated (Cu,Mo)-12s2 samples, s = 2 (●) and s = 3 (○), plotted against the average ionic radius, r(Ce^{IV},R^{III}), of the fluorite-block cations.

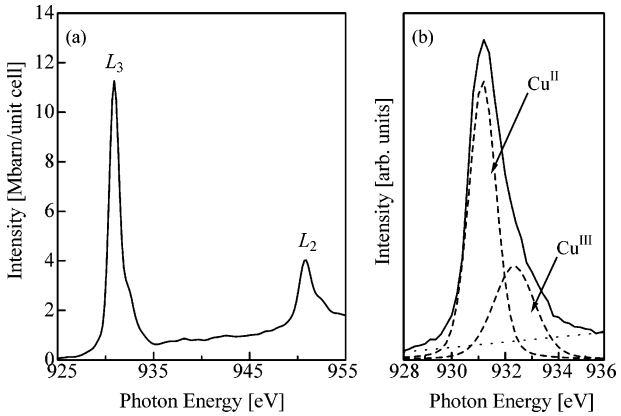

Figure 3. (a) Representative Cu $L_{2,3}$-edge XANES spectrum obtained for the superconductive (Cu,Mo)-1222 [$(Cu_{0.75}Mo_{0.25})Sr_2(Ce_{0.45}R_{0.55})_2Cu_2O_{9+\delta}$] samples (here R = Yb) and (b) illustration of the fitting of the spectral features (in the L_3 area) into Cu^{II} and Cu^{III} components.

both systems against r(Ce^{IV},R^{III}). The two systems (Cu,Mo)-1222 and (Cu,Mo)-1232 show essentially parallel trends. That is, with decreasing size of the R constituent, T_c first monotonically increases and then decreases, having a maximum at R = Y (i.e., at r(Ce^{IV},R^{III}) ≈ 0.99 Å).

Figure 3a displays a representative Cu $L_{2,3}$ spectrum obtained for the (Cu,Mo)-1222-phase samples (shown here for the smallest R constituent, Yb). The Cu L_3 area has been commonly used for the estimation of the average valence

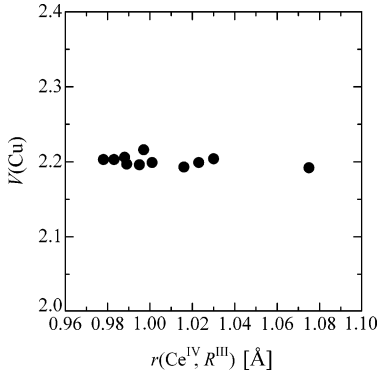

Figure 4. Average valence of copper, V(Cu), as estimated from Cu L_3-edge XANES data and plotted against the average ionic radius, r(Ce^{IV},R^{III}), for the superconductive (Cu,Mo)-1222 [$(Cu_{0.75}Mo_{0.25})Sr_2(Ce_{0.45}R_{0.55})_2Cu_2O_{9+\delta}$] samples.

state of copper in HTS copper oxides.[14,15,17,20−24] The narrow peak centered about 931.2 eV is due to divalent copper, Cu^{II} [i.e., transitions from the $Cu(2p_{3/2})3d^9$ ground state to the $Cu(2p_{3/2})^{-1}3d^{10}$ excited state, where $(2p_{3/2})^{-1}$ denotes a $2p_{3/2}$ hole], whereas the high-energy shoulder around 932.4 eV is assigned to trivalent copper states, Cu^{III} [i.e., transitions from the $Cu(2p_{3/2})3d^9\underline{L}$ ground state into the $Cu(2p_{3/2})^{-1}3d^{10}\underline{L}$ excited state, where $\underline{L}$ denotes a ligand hole in the O 2p orbital]. The spectral features about the Cu L_3 edge were analyzed following refs 14, 15, 21, and 24. In brief, the background, fitted with a straight line, was subtracted from the spectra, after which the fitting of the ∼931.2 eV (Cu^{II}) and ∼932.4 (Cu^{III}) peaks was done using combined Lorentzian and Gaussian functions; see Figure 3b for an illustration. From the integrated intensities of the two peaks an estimation for the average valence of copper was then obtained as V(Cu) ≡ 2 + I(Cu^{III})/[I(Cu^{II}) + I(Cu^{III})].[14,15,21,24] In Figure 4, the V(Cu) value is plotted against r(Ce^{IV},R^{III}) for the (Cu,Mo)-1222 samples. From Figure 4, it may be concluded that V(Cu) remains constant at 2.20 ± 0.01 within the entire R substitution range, just in a manner required for an ideal chemical-pressure system.

Then, O K-edge XANES spectroscopy was employed to see how the (excess) positive charge about copper is distributed between the two crystallographically distinct Cu-containing layers, i.e., the $(Cu,Mo)O_{1+\delta}$ charge reservoir and the CuO_2 plane. Representative O K-edge spectra (in the low-energy preedge energy range of 525−537 eV) for selected samples (of R = Yb, Y, and La) are displayed in Figure 5a. Three preedge peaks are distinguished. Two of them are straightforwardly assigned on the basis of the accumulated knowledge on various HTS copper oxide phases.[15,17,22−24]

(20) Bianconi, A.; De Santis, M.; Di Cicco, A.; M. Flank, A.; Fontaine, A.; Lagarde, P.; Katayama-Yoshida, H.; Kotani, A.; Marcelli, A. *Phys. Rev. B* **1988**, *38*, 7196.
(21) Ghigna, P.; Spinolo, G.; Flor, G.; Morgante, N. *Phys. Rev. B* **1998**, *57*, 13426.
(22) Nücker, N.; Pellegrin, E.; Schweiss, P.; Fink, J.; Molodtsov, S. L.; Simmons, C. T.; Kaindl, G.; Frentrup, W.; Erb, A.; Müller-Vogt, G. *Phys. Rev. B* **1995**, *51*, 8529.
(23) Merz, M.; Nücker, N.; Schweiss, P.; Schuppler, S.; Chen, C. T.; Chakarian, V.; Freeland, J.; Idzerda, Y. U.; Kläser, M.; Müller-Vogt, G.; Wolf, Th. *Phys. Rev. Lett.* **1998**, *80*, 5192.
(24) Schneider, M.; Unger, R.-S.; Mitdank, R.; Müller, R.; Krapf, A.; Rogaschewski, S.; Dwelk, H.; Janowitz, C.; Manzke, R. *Phys. Rev. B* **2005**, *72*, 014504.

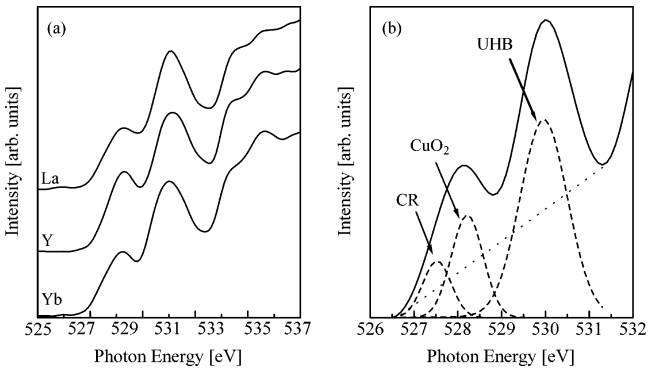

Figure 5. (a) Representative O K-edge XANES spectra obtained for the superconductive (Cu,Mo)-1222 [$(Cu_{0.75}Mo_{0.25})Sr_2(Ce_{0.45}R_{0.55})_2Cu_2O_{9+\delta}$] samples (here R = Yb, Y, and La) and (b) illustration of the fitting of the spectral features (in the preedge area) into components that correspond to hole states in the (Cu,Mo)$O_{1+\delta}$ charge reservoir (CR), superconductive CuO_2 planes, and the upper Hubbard band (UHB).

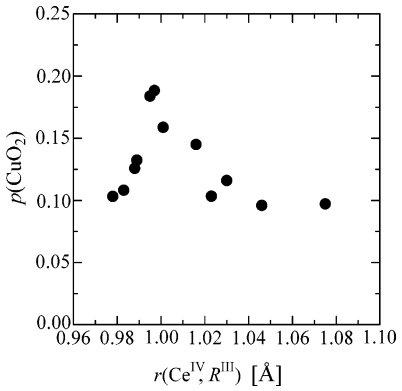

Figure 6. Density of CuO_2 plane holes, $p(CuO_2)$, plotted against the average ionic radius, $r(Ce^{IV},R^{III})$, for the superconductive (Cu,Mo)-1222 [$(Cu_{0.75}Mo_{0.25})Sr_2(Ce_{0.45}R_{0.55})_2Cu_2O_{9+\delta}$] samples. For the estimation of the $p(CuO_2)$ value, see the text.

The broad peak about ~530 eV is due to transitions into the upper Hubbard band (predominantly formed by the hybridization in the ground state of the $Cu3d^9$ and $Cu3d^{10}\underline{L}$ states), and the peak with a maximum at ~528.3 eV is due to the excitations of O 1s electrons to O 2p holes located in the CuO_2 planes. Partly overlapping with the latter peak, the third preedge peak is discerned at ~527.5 eV. With analogy to the Cu-1212 or $CuBa_2YCu_2O_{7-\delta}$ phase that also contains Cu in the charge-reservoir block,[22,23] we assign the 527.5 eV peak to the hole states at the oxygen sites in the (Cu,Mo)-$O_{1+\delta}$ charge-reservoir block. To derive a quantitative estimation for the distribution of holes between the (Cu,Mo)$O_{1+\delta}$ charge reservoir and the CuO_2 planes, we analyzed the spectral features by fitting the three preedge peaks with a combination of Lorentzian and Gaussian functions after approximating the background within 527−532 eV with a straight line; see Figure 5b. The thus obtained integrated intensities I(527.5) and I(528.3) of the two peaks at ~527.5 and ~528.3 eV are believed to be proportional to the relative hole densities of the (Cu,Mo)$O_{1+\delta}$ charge reservoir and the two CuO_2 planes, respectively. Hence, the ratio $0.5I(528.3)/[I(528.3) + I(527.5)]$ should give us the share of one CuO_2 plane of the total hole content. For the total hole content (p), on the other hand, we obtain a reasonable estimate from the Cu L-edge XANES data, i.e., $p \equiv 2.75\ [V(\mathrm{Cu})-2]$. Hence, we calculate an estimate for the absolute CuO_2 plane hole density [$p(CuO_2)$] as follows: $p(CuO_2) \equiv 0.5[I(528.3)]\text{-}p/[I(528.3) + I(527.5)]$. Note that a common V(Cu) value of 2.20 was used for all the samples. In Figure 6, we plot the thus obtained $p(CuO_2)$ values against $r(Ce^{IV},R^{III})$. It is immediately recognized that the $p(CuO_2)$ versus $r(Ce^{IV},R^{III})$ plot is almost identical with the T_c versus $r(Ce^{IV},R^{III})$ plot (shown for the same samples in Figure 2), suggesting that the chemical-pressure-derived changes in T_c are simply due to changes in the CuO_2 plane hole density. Since the total amount of holes remains constant, this means that for the larger R constituents holes are gradually shifted from the (Cu,Mo)$O_{1+\delta}$ charge reservoir to the CuO_2 planes upon decreasing the size of the R constituent, whereas for the smaller R constituents the direction of the hole shift is opposite.

Hence, we have so far shown that the size of the R constituent apparently has an influence on the charge distribution between the nonsuperconductive charge-reservoir block and the superconductive CuO_2 planes. Assuming that the situation for the Cu-1212 ($CuBa_2RCu_2O_{7-\delta}$) and Cu-2212 ($Cu_2Ba_2RCu_2O_{8-\delta}$) systems would be parallel to that for the (Cu,Mo)-1222 system with the large R constituents, i.e., a decrease in $r(R^{III})$ would increase $p(CuO_2)$, we propose an explanation for the different T_c versus $r(R^{III})$ behaviors of the Cu-1212 and Cu-2212 systems. Fully oxygenated Cu-1212 superconductors are in a slightly overdoped state. Therefore, an increase in $p(CuO_2)$ upon decreasing $r(R^{III})$ decreases the value of T_c. On the other hand, Cu-2212 superconductors are known to be underdoped (unless R^{III} is partly substituted by divalent calcium). This is why T_c increases with decreasing $r(R^{III})$ and increasing $p(CuO_2)$. Coming back to the present (Cu,Mo)-1222 and (Cu,Mo)-1232 systems, from our previous studies we believe them to be underdoped.[13,14] Hence, for the larger R constituents the trend of increasing T_c with decreasing $r(R^{III})$ [and increasing $p(CuO_2)$] is just what we should expect provided that the (Cu,Mo)-1222 and (Cu,Mo)-1232 systems behave in the same way as the Cu-1212 and Cu-2212 systems. Then the only question left open is why the trend of increasing $p(CuO_2)$ with decreasing $r(Ce^{IV},R^{III})$ abruptly changes about R = Y for (Cu,Mo)-1222 and (Cu,Mo)-1232. Here we acknowledge the importance of precise crystal structure analysis. On the basis of the present XRD data collected by commercial laboratory equipment, it was not possible to address the aforementioned question.

Conclusion

We have utilized the $s = 2$ and 3 members of the recently established (Cu,Mo)-12s2 homologous series as a novel model system to deepen our understanding of rare-earth-derived chemical-pressure effects in layered copper oxide superconductors. Superconductive samples with 11 different R constituents from La to Yb in the fluorite-structured $(Ce,R)[O_2(Ce,R)]_{s-1}$ block separating the adjacent CuO_2 planes were successfully synthesized. It was shown that the size of the R constituent has a significant influence on the charge distribution between the nonsuperconductive charge-

reservoir block and the superconductive CuO_2 planes. To follow these changes, O K-edge XANES spectroscopy was utilized. The total amount of holes was determined from Cu L-edge XANES data. For samples with the same amount of holes in total, the value of T_c was found to show a rather interesting behavior, increasing first with decreasing size of the R constituent up to R = Y and then showing just an opposite trend for the smallest R constituents. It however turned out that the changes in T_c were fully explained by the observed changes in the CuO_2 plane hole density. Finally, it is emphasized that the results revealed for the members of the (Cu,Mo)-12*s*2 series could be readily extended to explain the chemical-pressure effects in the two well-known R-based HTS copper oxide systems Cu-1212 and Cu-2212.

Acknowledgment. This work was supported by a Grant-in-Aid for Scientific Research (No. 15206002) from the Japan Society for the Promotion of Science and also by the Academy of Finland (Decision Nos. 110433 and 116254). I.G. acknowledges a scholarship (ID 043145) from the Ministry of Education, Culture, Sports, Science and Technology of Japan, and R.S.L. thanks the National Science Council for financial support (Contract No. NSC 95-2113-M-002-009).

CM061856R